PHYSICAL REVIEW C VOLUME 59, NUMBER 1 JANUARY 1999

Canonical treatment of fluctuations and random phase approximation correlations at finite temperature

N. Canosa,[1,2] R. Rossignoli,[1,2] and P. Ring[2]
[1]Departamento de Física, Universidad Nacional de La Plata, c.c. 67, 1900 La Plata, Argentina
[2]Physik-Department der Technischen Universität München, D-85748 Garching, Germany
(Received 17 August 1998)

The static path plus random phase approximation (SPA+RPA) to the partition function is formulated exactly in a canonical ensemble, for the case of a density decomposition of an arbitrary two-body Hamiltonian. The canonical mean field plus RPA approach is also discussed. Numerical results are shown for a quadrupole interaction, where excellent agreement with the exact canonical results for a light nucleus is obtained. An effective canonical mean field plus RPA approach is in this case also developed, which avoids the sharp phase transition of the ordinary mean field and provides a reliable estimate of full SPA+RPA results. [S0556-2813(99)02901-5]

PACS number(s): 21.60.Jz, 24.60.Ky, 21.60.Cs, 05.30.−d

I. INTRODUCTION

The path integral representation of the partition function (PF) obtained with the Hubbard Stratonovich transformation [1] constitutes a powerful tool for describing strongly correlated finite Fermi systems at finite temperature. In particular, the static path approximation (SPA) [2–6], obtained by considering just time-independent fields in the path integral, provided for the first time a fully microscopic treatment of large amplitude statistical shape and pairing fluctuations in hot nuclei [4], which had been previously introduced in a qualitative way by means of semimacroscopic Landau-type prescriptions [7–9]. These fluctuations are essential for describing the strong attenuation, due to finite size effects, of the sharp phase transitions exhibited by the thermal mean field approximations. The SPA+RPA approach [10–15], to be denoted for brevity as correlated (C) SPA, includes in addition small amplitude quantumlike fluctuations and is able to yield a very accurate evaluation of the PF for a wide range of temperatures, improving the SPA at low temperatures and providing in principle an alternative to Monte Carlo–type evaluations of the full path integral [16,17], at least for effective interactions with a few separable terms. The CSPA was recently extended to the evaluation of strength functions [13,15] and adapted to deal with repulsive forces [14].

The SPA and CSPA were originally derived in the grand canonical (GC) ensemble [10–13], which involves statistical fluctuations in the particle number. These become non-negligible in small systems such as finite nuclei, where a *canonical* ensemble with fixed proton and neutron particle number is in principle required for a correct description of thermodynamic averages [18]. In this work we rigorously formulate, in Sec. II, the full CSPA in a canonical ensemble, for a densitylike decomposition of an arbitrary two-body interaction. In addition, we derive the mean field plus RPA treatment [19] in a canonical ensemble, obtained as the saddle point approximation to the CSPA. This approach, though unable to avoid the sharp phase transition of the mean field, may in principle provide a reliable estimate of the PF well away from transitional regions with minimum numerical effort and deserves consideration. We should mention that both exact and approximate canonical SPA treatments (i.e., without the effects of quantum fluctuations) were previously considered in Refs. [6,18].

In Sec. III the present methods are applied to a quadrupole-quadrupole interaction, where comparison with exact canonical results is made for a light deformed nucleus within the *s-d* shell. We also derive in this case an *effective* mean field+RPA approach, which includes the RPA correlations in the treatment of Ref. [20] and extends it to a canonical ensemble. This approach avoids the sharp deformed to spherical transition of the conventional mean field and is able to reproduce full CSPA results for most observables with good accuracy. Conclusions are finally drawn in Sec. IV.

II. FORMALISM

A. Canonical CSPA

We consider a Hamiltonian of the form

$$H=H_0-\tfrac{1}{2}\sum_\nu v_\nu Q_\nu^2, \tag{1}$$

where H_0 and Q_ν are standard one-body operators

$$Q_\nu=\sum_{k,k'} Q^\nu_{kk'}c^\dagger_k c_{k'}\,. \tag{2}$$

Equation (1) corresponds then to a particular density decomposition of an arbitrary two-body interaction [16]. We start from the auxiliary field path integral representation of the PF obtained with the Hubbard-Stratonovich transformation [1]

$$Z=\int D[x]\mathrm{Tr}\,\hat{T}\exp\left\{-\int_0^\beta d\tau H[x(\tau)]\right\}, \tag{3}$$

$$H(x)=H_0+\sum_\nu \frac{x_\nu^2}{2v_\nu}-x_\nu Q_\nu\,, \tag{4}$$

where $\hat{T}$ denotes the time ordering operator, $\beta=T^{-1}$, and $H(x)$ is a linearized *one-body* Hamiltonian. Employing a Fourier expansion of $x(\tau)$ in the interval $[0,\beta]$

$$x_\nu(\tau)=x_\nu+\sum_{n\neq 0} x_n^\nu e^{i\omega_n\tau}, \quad \omega_n=2\pi n/\beta, \tag{5}$$

Eq. (3) can be expressed as an integral over the coefficients x_ν, x_n^ν. Here $x_\nu\equiv x_0^\nu$ denotes the *static* coefficients, which represent the time average of $x_\nu(\tau)$ in $[0,\beta]$. In the CSPA, one retains the exact integration over x_ν, in order to take into account large amplitude static fluctuations, while the remaining coefficients are integrated out in the saddle point approximation for each value of x_ν. The last step includes small amplitude quantumlike fluctuations which account for the RPA correlations. The final result can be cast as [10,13,14]

$$Z_{\rm CSPA}=\int d(x)Z(x)C_{\rm RPA}(x), \tag{6}$$

where $d(x)=\Pi_\nu(2\pi v_\nu/\beta)^{-1/2}dx_\nu$ and

$$Z(x)=\mathrm{Tr}\,\exp[-\beta H(x)], \tag{7}$$

$$C_{\rm RPA}(x)=\prod_{n=1}^{\infty}\mathrm{Det}[\delta_{\nu\nu'}+v_\nu R_{\nu\nu'}(x,i\omega_n)]^{-1} \tag{8}$$

$$=\prod_{\alpha>0}\frac{\omega_\alpha\sinh[\beta\varepsilon_\alpha/2]}{\varepsilon_\alpha\sinh[\beta\omega_\alpha/2]}. \tag{9}$$

Here $R_{\nu\nu'}(x,\omega)$ is a thermal response matrix, which, in the running single particle (SP) basis where $H(x)$ is diagonal, i.e.,

$$H(x)=\varepsilon_0+\sum_k \varepsilon_k a_k^\dagger a_k, \quad a_k^\dagger=\sum_{k'} W_{k'k}c_{k'}^\dagger, \tag{10}$$

$$Q_\nu=\sum_{k,k'}\tilde{Q}^\nu_{kk'}a_k^\dagger a_{k'}, \quad \tilde{Q}^\nu_{kk'}=[W^\dagger Q^\nu W]_{kk'}, \tag{11}$$

with $\varepsilon_0=\Sigma_\nu x_\nu^2/2v_\nu$, can be expressed as

$$R_{\nu\nu'}(x,\omega)=\sum_{k\neq k'}\tilde{Q}^\nu_{kk'}\tilde{Q}^{\nu'}_{k'k}\frac{p_k-p_{k'}}{\varepsilon_k-\varepsilon_{k'}+\omega}$$

$$=\sum_\alpha \tilde{Q}^\nu_\alpha\tilde{Q}^{\nu'*}_\alpha\frac{p_\alpha}{\varepsilon_\alpha+\omega}, \tag{12}$$

where α denotes all pairs $k\neq k'$, with $\varepsilon_\alpha\equiv\varepsilon_k-\varepsilon_{k'}$, $p_\alpha\equiv p_k-p_{k'}$ and

$$p_k=\langle a_k^\dagger a_k\rangle_x=-\beta^{-1}\partial\ln Z(x)/\partial\varepsilon_k, \tag{13}$$

the SP occupation probabilities. In Eq. (9), $\omega_\alpha(x)$ are the *finite temperature RPA energies* around $H(x)$, defined as the eigenvalues of

$$A_{\alpha\alpha'}(x)=\varepsilon_\alpha\delta_{\alpha\alpha'}+p_\alpha\sum_\nu v_\nu\tilde{Q}^{\nu*}_\alpha\tilde{Q}^\nu_{\alpha'}, \tag{14}$$

which can be determined as the roots of

$$\mathrm{Det}[\delta_{\nu\nu'}+v_\nu R_{\nu\nu'}(x,\omega_\alpha)]=0 \tag{15}$$

for the nontrivial cases $\omega_\alpha\neq\varepsilon_\alpha$.

Equation (6) can in principle be applied if $C_{\rm RPA}(x)>0\,\forall x$. This determines a breakdown temperature, normally very low, below which it is no longer applicable due to the appearance of imaginary RPA energies with $\beta|\omega_\alpha(x)|>2\pi$ at unstable values of x, where the small amplitude approximation for the quantum fluctuations no longer holds. The SPA is obtained if the factor $C_{\rm RPA}(x)$ is neglected. Within a finite configuration space, the SPA coincides with the CSPA at high temperatures, where $C_{\rm RPA}(x)\to 1-(\beta^2/24)\Sigma_\alpha\omega_\alpha^2-\varepsilon_\alpha^2$, with p_α (and hence $\omega_\alpha-\varepsilon_\alpha$) of order β.

All previous expressions are general and can be applied in *both the grand canonical and canonical ensembles*, as the expression (12) for the response matrix is valid in both cases if $[Q_\nu,N]=0$, $[H_0,N]=0$ (see Appendix A). Only $Z(x)$ and p_k will be different. In the GC case, we should obviously add a term $-\mu N$ to $H(x)$ and Eq. (13) becomes the usual Fermi probability.

In the *canonical* case, we may evaluate the PF for N particles as

$$Z_N(x)=\frac{1}{2\pi i}\oint dz\frac{Z(x,z)}{z^{N+1}}, \tag{16}$$

where the integration path encloses the origin and

$$Z(x,z)=\mathrm{Tr}\,z^{\hat{N}}\exp[-\beta H(x)]=\sum_N z^N Z_N(x)$$

$$=e^{-\beta\varepsilon_0}\prod_k[1+ze^{-\beta\varepsilon_k}], \tag{17}$$

is the GC PF, with $z=e^{\beta\mu}$. The canonical probability (13) becomes

$$p_k=\frac{1}{2\pi i Z_N(x)}\oint dz\frac{Z(x,z)p_k(z)}{z^{N+1}}, \tag{18}$$

$$p_k(z)=[1+z^{-1}e^{\beta\varepsilon_k}]^{-1}, \tag{19}$$

where $p_k(z)$ is the Fermi probability. Equation (16) can be explicitly evaluated as

$$Z_N(x)=\frac{1}{2\pi}\int_{-\pi}^{\pi}(z_0e^{i\alpha})^{-N}Z(x,z_0e^{i\alpha})d\alpha \tag{20}$$

$$=\frac{1}{L+1}\sum_{j=-L/2}^{L/2}(z_0e^{i\alpha_j})^{-N}Z(x,z_0e^{i\alpha_j}),$$

$$\alpha_j=\frac{2\pi j}{L+1}, \tag{21}$$

where Eq. (21) holds in a finite SP configuration space of dimension L for $0 \leqslant N \leqslant L$, and z_0, in principle an arbitrary constant, is to be close for numerical feasibility to the value determined by the constraint

$$\sum_k p_k(z_0) = N, \tag{22}$$

which fixes z in the GC ensemble and determines the maximum of $z^{-N}Z(x,z)$. In this way, the integrand in Eq. (20) acquires an approximate Gaussian shape around $z = z_0$ and cancellations are avoided. In fact, for not too low temperatures (i.e., larger than half the average SP level spacing) Eqs. (20), (21) can be accurately evaluated in the stationary phase approximation [18],

$$Z_N(x) \approx z_0^{-N} Z(x,z_0)/(2\pi\sigma_N^2)^{1/2}, \tag{23}$$

$$\sigma_N^2 = \sum_k p_k(z_0)[1 - p_k(z_0)], \tag{24}$$

where σ_N^2 is the GC number fluctuation and z_0 the value determined by Eq. (22). We should mention that the canonical PF may also be evaluated by means of recursive methods [21].

If the decomposition (1) is such that $[Q_\nu, N_\tau] = 0$, $[H_0, N_\tau] = 0$, where N_τ, $\tau = p,n$, denote the proton and neutron number operators, the whole formalism can be applied in a canonical ensemble with fixed N_p and N_n. In this case $H(x) = H_p(x) + H_n(x)$ and

$$Z(x) = Z_{N_p}(x) Z_{N_n}(x), \tag{25}$$

where the canonical PF $Z_{N_\tau}(x)$ for proton or neutron can be obtained with the previous methods.

B. Canonical mean field+RPA

Let us consider now the full saddle point approximation to Eq. (3), where all variables, including the static coefficients, are integrated in the Gaussian approximation around a (static) stationary point of the integrand. These are determined by the self-consistent equations

$$x_\nu = v_\nu \langle Q_\nu \rangle_x, \quad \langle Q_\nu \rangle_x = \sum_k \tilde{Q}^\nu_{kk} p_k, \tag{26}$$

which represent the finite temperature Hartree equations *in both the GC or canonical ensembles*. The type of statistics is determined by p_k. At a solution of Eq. (26), $Z(x)$ becomes the Hartree PF. The full saddle point approximation around this point leads to the mean field+RPA (CMFA) PF,

$$Z_{\text{CMFA}} = Z(x) C_0(x) C_{\text{RPA}}(x), \tag{27}$$

where [see Eqs. (A2),(A3)]

$$C_0(x) = \mathrm{Det}[\delta_{\nu\nu'} + v_\nu R^0_{\nu\nu'}(x)]^{-1/2}, \tag{28}$$

$$R^0_{\nu\nu'}(x) \equiv -\frac{\partial \langle Q_\nu \rangle_x}{\partial x_{\nu'}} = \sum_{k \neq k'} \tilde{Q}^\nu_{kk'} \tilde{Q}^{\nu'}_{k'k} \frac{p_k - p_{k'}}{\varepsilon_k - \varepsilon_{k'}} - \beta \sum_{k,k'} \tilde{Q}^\nu_{kk} \tilde{Q}^{\nu'}_{k'k'} C_{kk'}, \tag{29}$$

with $C_{kk'}$ the correlation

$$C_{kk'} = -\frac{1}{\beta}\frac{\partial p_k}{\partial \varepsilon_{k'}} = \langle a_k^\dagger a_k a_{k'}^\dagger a_{k'} \rangle_x - p_k p_{k'} = \delta_{\tau_k \tau_{k'}} \left[\delta_{kk'} p_k + (1 - \delta_{kk'}) \frac{p_k e^{\beta\varepsilon_k} - p_{k'} e^{\beta\varepsilon_{k'}}}{e^{\beta\varepsilon_k} - e^{\beta\varepsilon_{k'}}} - p_k p_{k'} \right]. \tag{30}$$

Equation (30) is valid for $\varepsilon_k \neq \varepsilon_{k'}$ (see Appendix B) and holds in both the canonical and GC ensembles, but in the latter reduces to $C_{kk'} = \delta_{kk'} p_k(1 - p_k)$, whereas in the canonical case off diagonal terms do not vanish. Note that

$$(p_k - p_{k'})/(\varepsilon_k - \varepsilon_{k'}) \to \beta[C_{kk'} - p_k(1 - p_k)]$$

in Eq. (29) for $\varepsilon_k \to \varepsilon_{k'}$, as seen from Eq. (30). Equation (29) differs from the limit of the response matrix (12) for $\omega \to 0$ due to the last sum in Eq. (29), which contains the diagonal terms stemming from the variations of the probabilities p_k. In a basis where $\tilde{Q}^{\nu'}_{kk'} = \delta_{kk'} \tilde{Q}^{\nu'}_{kk}$ if $\varepsilon_k = \varepsilon_{k'}$, we can rewrite Eq. (29) as

$$R^0_{\nu\nu'}(x) = R_{\nu\nu'}(x,0) - \sum_k \frac{\partial p_k}{\partial x_{\nu'}} \tilde{Q}^\nu_{kk}. \tag{31}$$

Equation (27) is strictly applicable only around a stable nondegenerate mean field. If the mean field solution breaks a continuous symmetry of H, it will exhibit a continuous degeneracy and the determinant in Eq. (28) will vanish. In these cases the static variables x_ν naturally include the reorientation of the mean field and the Gaussian approximation should be applied just to the ''intrinsic'' variables (see next section). The factor $C_0(x)$ will in any case diverge at the mean field phase transitions, so that the Gaussian approximation (27) will be reliable only well away from critical regions. It may nevertheless be employed to obtain exact asymptotic expressions for high T (see next section).

On the other hand, static variables associated with repulsive terms [$v_\nu < 0$ in Eq. (1) with Q_ν Hermitian, equivalent to $v_\nu > 0$ and Q_ν anti-Hermitian] can be treated within the CSPA in the present saddle point approximation (see Ref. [14]), which for these variables is always reliable except for very low temperatures (where in any case the CSPA is no longer applicable).

III. APPLICATION

We consider a quadrupole interaction

$$H = H_0 - \tfrac{1}{2}\chi Q^\dagger Q = H_0 - \tfrac{1}{2}\chi \sum_\mu Q^{r2}_\mu, \tag{32}$$

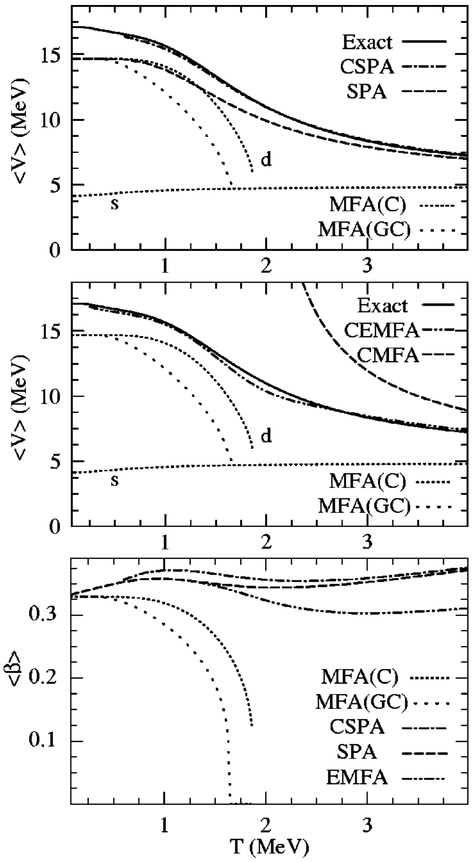

FIG. 1. The average quadrupole energy $\langle V\rangle=\frac{1}{2}\chi\langle Q^\dagger\cdot Q\rangle$ vs temperature for ^{20}Ne, according to canonical CSPA and SPA (top), and standard [CMFA, Eq. (42)] and effective [CEMFA, Eq. (49)] canonical mean field plus RPA (center). The exact canonical results, as well as canonical (C) and grand canonical (GC) mean field results (MFA) for the deformed (d) and spherical (s) solutions are also depicted. Bottom: Quadrupole deformation parameter in the canonical and grand canonical mean field approximations, and average potential deformation in the canonical CSPA and SPA. The deformation obtained from the effective mean field Eqs. (48) is also depicted (EMFA).

$$Q_0^r=Q_0,\quad Q^r_{\pm\mu}=\binom{1}{i}\frac{Q_\mu\pm Q_\mu^\dagger}{\sqrt{2}},\quad \mu=1,2, \tag{33}$$

where H_0 is a spherical SP Hamiltonian, Q_μ quadrupole SP operators, and Q^r_μ the Hermitian partners.

A. CSPA

Equation (6) will lead in this case to a five-dimensional integral over variables $x=\{x_\mu\}$, which includes all possible orientations of the deformed linearized SP Hamiltonian

$$H(x)=H_0-\sum_\mu \frac{x_\mu^2}{2\chi}-x_\mu Q^r_\mu. \tag{34}$$

The CSPA PF can then be written as

$$Z_{\rm CSPA}=\frac{1}{(2\pi\chi T)^{5/2}}\int d^5x Z(x)C_{\rm RPA}(x) \tag{35}$$

$$=\frac{1}{2\pi\chi T}\frac{1}{6}\int_{-\infty}^{\infty}d\tilde{x}_0\int_{-\infty}^{\infty}d\tilde{x}_2\, m(\tilde{x})Z(\tilde{x})C_{\rm RPA}(\tilde{x}), \tag{36}$$

where in Eq. (36) we integrated out the orientation variables, with $\tilde{x}_\mu=0$ for $\mu=\pm1,-2$ and

$$m(\tilde{x})=\sqrt{\frac{2\pi}{(\chi T)^3}}|\tilde{x}_2(3\tilde{x}_0^2-\tilde{x}_2^2)|, \tag{37}$$

the ensuing ''intrinsic'' measure fulfilling

$$\frac{1}{2\pi\chi T}\frac{1}{6}\int_{-\infty}^{\infty}d\tilde{x}_0\int_{-\infty}^{\infty}d\tilde{x}_2 m(\tilde{x})e^{-(\tilde{x}_0^2+\tilde{x}_2^2)/2\chi T}=1. \tag{38}$$

Setting $(\tilde{x}_0,\tilde{x}_2)=\hbar\omega\beta(\cos\gamma,\sin\gamma)$, we recover the ordinary quadrupole deformation parameters β,γ, with

$$H(\tilde{x})=H_0+\frac{\beta^2}{2\chi'}-\hbar\omega\beta(\cos\gamma Q_0^r+\sin\gamma Q_2^r), \tag{39}$$

$$\frac{1}{2\pi\chi T}m(\tilde{x})d\tilde{x}_0 d\tilde{x}_2=\frac{1}{\sqrt{2\pi(\chi' T)^5}}\beta^4|\sin 3\gamma|d\beta d\gamma, \tag{40}$$

where $\chi'=\chi/(\hbar\omega)^2$. In the absence of rotational frequency the integral (36) can be reduced to the sector $0\leqslant\gamma\leqslant\pi/3$, $\beta>0$, i.e., $0\leqslant\tilde{x}_2\leqslant\sqrt{3}\tilde{x}_0$, $\tilde{x}_0>0$, with a multiplicity factor 6. The factor $C_{\rm RPA}(\tilde{x})$ is to be evaluated with the full response matrix (29) constructed with all five operators Q^r_μ. In what follows β will denote the deformation parameter.

B. Conventional mean field+RPA

Equation (35) takes into account both shape and orientation fluctuations around the mean field, determined by the equations

$$x_\mu=\chi\langle Q^r_\mu\rangle_x, \tag{41}$$

which imply the identity of potential and density deformations. The *spherical* nondegenerate solution $x_\mu=0\,\forall\mu$ will be the unique solution at sufficiently high $T(T>T_c)$. The ensuing CMFA PF (27) is obtained in this case integrating Eq. (35) in the Gaussian approximation around the origin,

$$Z_{\rm CMFA}=Z(0)C_0(0)C_{\rm RPA}(0),\quad T>T_c, \tag{42}$$

where all quantities are evaluated for $H(x)=H_0$, with

$$C_0(0)={\rm Det}[\delta_{\mu\mu'}+\chi R^0_{\mu\mu'}(0)]^{-1/2}, \tag{43}$$

and μ,μ' running over all five indexes. Equation (42) will not be reliable for T near T_c, but provides nevertheless exact asymptotic expressions for high T. In this limit we may neglect $C_{\rm RPA}(0)$ in Eq. (42), i.e.,

$$Z_{\rm CMFA}\approx Z(0)C_0(0),\quad T\gg T_c, \tag{44}$$

which is just the Gaussian approximation to the SPA.

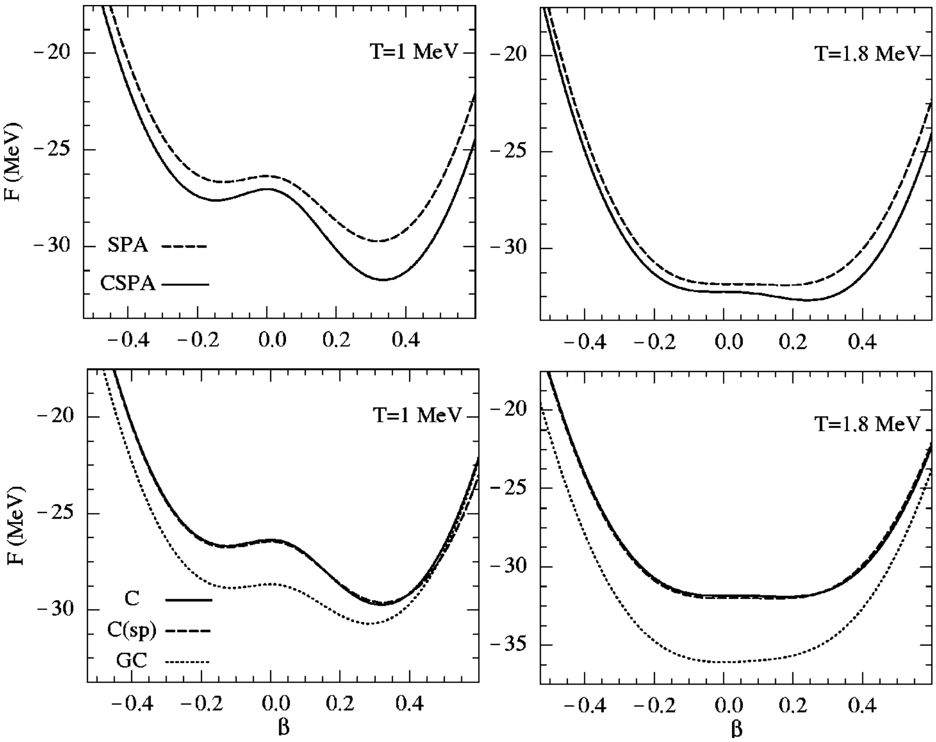

FIG. 2. Top: The SPA and CSPA free energy potentials (53), (54) vs deformation for $\gamma=0$ at the indicated temperatures. Bottom: Comparison between the canonical (C) and grand canonical (GC) SPA potentials (53) and (56). C(SP) depicts the saddle point approximation (55).

On the other hand, the deformed solutions ($x\neq 0$) of Eq. (41) are continuously degenerate, representing reorientations of the solutions of the intrinsic equations

$$\tilde{x}_\mu=\chi\langle Q^r_\mu\rangle_{\tilde{x}}, \quad \mu=0,2. \tag{45}$$

This entails the vanishing of the determinant in Eq. (28) when taken with respect to all five variables, as well as of the lowest RPA energies determined by Eq. (15) (Goldstone modes [22]). One could attempt a naive saddle point approximation in the *intrinsic* variables of Eq. (36), which would lead to

$$Z_{\mathrm{CMFA}}=Z(\tilde{x})m(\tilde{x})C^i_0(\tilde{x})C_{\mathrm{RPA}}(\tilde{x}), \quad T<T_c, \tag{46}$$

$$C^i_0(\tilde{x})=\mathrm{Det}[\delta_{\mu\mu'}+\chi R^0_{\mu\mu'}(\tilde{x})]^{-1/2}, \quad \mu,\mu'=0,2, \tag{47}$$

where $\tilde{x}$ is a deformed solution of Eq. (45), but unfortunately, Eq. (46) is feasible only for a triaxial solution, as $m(\tilde{x})$ vanishes for the normal case of axially symmetric solutions (prolate or oblate). An alternative effective mean field+RPA which takes into account the important effects of the measure in Eq. (36) is discussed below.

C. Effective mean field +RPA

The maximum of $Z(\tilde{x})m(\tilde{x})$ is determined by the equation

$$\tilde{x}_\mu=\chi\langle Q^r_\mu\rangle_{\tilde{x}}+\chi T\frac{\partial \ln m(\tilde{x})}{\partial\tilde{x}_\mu}, \quad \mu=0,2 \tag{48}$$

whose solution is nonspherical (nor axial) at any temperature as $m(\tilde{x})$ vanishes in these cases. The sharp deformed to spherical transition of the ordinary mean field is thus avoided [20]. The solution of Eq. (48) represents approximately the average SPA intrinsic *potential* deformations $\langle\tilde{x}_\mu\rangle$ [20], and approaches the ordinary mean field for $T\rightarrow 0$. The full Gaussian approximation around this solution yields

$$Z_{\mathrm{CEMFA}}=Z(\tilde{x})m(\tilde{x})C'^i_0(\tilde{x})C_{\mathrm{RPA}}(\tilde{x}), \tag{49}$$

$$C'^i_0(\tilde{x})=\mathrm{Det}\left[\delta_{\mu\mu'}+\chi R^0_{\mu\mu'}(\tilde{x})-\chi T\frac{\partial^2\ln m(\tilde{x})}{\partial\tilde{x}_\mu\partial\tilde{x}_{\mu'}}\right]^{-1/2},$$

with $\mu,\mu'=0,2$. Equation (49) remains normally stable for all temperatures with $C'^i_0(\tilde{x})>0\forall T$. Accurate estimates of the PF and its first derivatives can be obtained just from Eq. (49) as will be seen below. Moreover, Eq. (49) can be extended to temperatures lower than in the CSPA, as configurations well away from the mean field are avoided at low T. Nonetheless, there may still exist a breakdown temperature if the lower RPA energy is complex at the effective mean field.

D. Results

Numerical results for ^{20}Ne in the *s-d* shell are shown in Figs. 1–5, where the *exact* canonical PF has been calculated by a full diagonalization of the Hamiltonian (32). We employed the SP energies (all quantities in MeV) $\varepsilon_{1/2}=-4.212$, $\varepsilon_{3/2}=0$, $\varepsilon_{5/2}=-5.083$, with $\chi=70/A^{1.4}$ and $\hbar\omega=41.2/A^{1/3}$. The RPA correction factor in the CSPA has been evaluated exactly in terms of the RPA energies using Eq. (9).

We first consider the average quadrupole energy $\frac{1}{2}\chi\langle Q^\dagger\cdot Q\rangle$, where

$$\langle Q^\dagger\cdot Q\rangle=Z^{-1}\mathrm{Tr}[\exp(-H/T)Q^\dagger\cdot Q]=2T\partial\ \ln Z/\partial\chi, \tag{50}$$

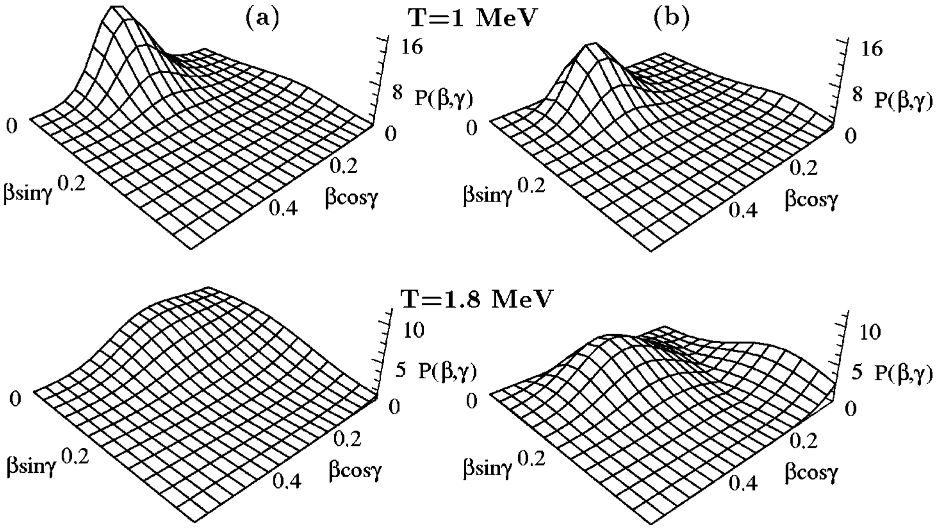

FIG. 3. The normalized distributions (57) for $\sigma=0$ (a) and $\sigma=1$ (b) at the indicated temperatures.

is the canonical average. The high T limit of this quantity can be obtained from Eqs. (43),(44), which lead to

$$\langle Q^{\dagger}\cdot Q\rangle \approx -T\sum_{\mu}\,[(1+\chi R^{0})^{-1}R^{0}]_{\mu\mu} \tag{51}$$

and hence to a non-negligible value of the difference $\langle Q^{\dagger}Q\rangle_{\chi}-\langle Q^{\dagger}Q\rangle_{\chi=0}$ even for T quite above T_c, which behaves as T^{-1} for high T. This is the fluctuation effect seen at the SPA level. At the mean field level, such difference obviously vanishes for $T>T_c$. Note that in a *canonical* mean field, Wick's theorem no longer holds and we should evaluate Eq. (50) as

$$\begin{aligned}\langle Q^{\dagger}\cdot Q\rangle_x &\equiv Z^{-1}(x)\mathrm{Tr}\{\exp[-H(x)/T]Q^{\dagger}\cdot Q\}\\ &=\langle Q^{\dagger}\rangle_x\cdot\langle Q\rangle_x\\ &\quad+\sum_{k,k'}\{Q^{\dagger}_{kk'}\cdot Q_{k'k}\,p_k(1-p_{k'})\\ &\quad+C_{kk'}[Q^{\dagger}_{kk}\cdot Q_{k'k'}-Q^{\dagger}_{kk'}\cdot Q_{k'k}]\},\end{aligned} \tag{52}$$

where the last line vanishes in a GC ensemble. For $T>T_c$, $x=0$ and $\langle Q\rangle_0=0$ but the sum in Eq. (52) does not vanish and approaches Eq. (51) for $\chi=0$ for $T\gg T_c$.

As seen in Fig. 1, the CSPA results for the quadrupole energy, obtained using Eq. (50) with the CSPA PF (36), are practically coincident with the exact ones for T above the CSPA breakdown ($T\approx 0.5$ MeV). There is an appreciable attenuation of the deformed to spherical transition present in the mean field approximations, as well as a non-negligible difference with the spherical average even for $T>3$ MeV. The canonical SPA results [here evaluated as the SPA average of Eq. (52) [6]] also provide the correct high T behavior, but the RPA correlations are important for an accurate agreement at low T. It is also seen that non-negligible differences exist between canonical and GC mean field results. In the canonical case the critical temperature is larger and the deformed to spherical transition is of first order type (see below).

It is actually remarkable that results obtained with the effective mean field + RPA, Eq. (49), are almost of the same accuracy as those of CSPA, as seen in the central panel, except for a narrow region around T_c. Moreover, Eq. (49) can be extended to lower temperatures, the breakdown occurring at $T\approx 0.15$ MeV. Results from the conventional spherical mean field+RPA, Eq. (42), although providing the correct high T limit, are not reliable even up to $T=4$ MeV and diverge at $T=T_c$, being in fact almost coincident with those from Eq. (44) as the RPA correction is small for $T>T_c$. The poor accuracy of Eq. (42) in this region reflects the flatness of the spherical maxima of $Z(x)$ (see below), which makes a conventional Gaussian evaluation inadequate.

In the bottom panel we plot the mean field deformations together with the CSPA and SPA average *potential* deformations. The latter remain roughly constant [note that for high T, $\langle\beta^2\rangle^{1/2}\rightarrow(5\chi' T)^{1/2}$ in the SPA or CSPA, as seen from Eq. (35)], which gives rise to large differences with the mean field predictions. The effective deformation $\beta=\sqrt{\tilde{x}_0^2+\tilde{x}_2^2}/\hbar\omega$ obtained from the solution of Eqs. (48) is close to the average SPA potential deformation, being almost coincident for low T.

In the top panel of Fig. 2 we depict the intrinsic free energy potentials

$$F_{\mathrm{SPA}}(\tilde{x})=-T\ln Z(\tilde{x}), \tag{53}$$

$$F_{\mathrm{CSPA}}(\tilde{x})=-T\,\ln[Z(\tilde{x})C_{\mathrm{RPA}}(\tilde{x})], \tag{54}$$

where $Z(\tilde{x})$ is the canonical PF, for $\gamma=0$ (oblate shapes $\beta>0,\gamma=\pi/3$ correspond of course to $\beta<0,\gamma=0$). The minimum of Eq. (53) determines the canonical mean field. At $T=1$ MeV, the SPA potential exhibits the expected double well shape with an absolute prolate minimum, while at $T=1.8$ MeV it becomes almost flat for $-0.2<\beta<0.3$, entailing large shape fluctuations. The RPA correction decreases the free energy $\forall\beta$ but its effect on the potential shape is rather small for T not too close to the breakdown. It slightly favors deformation, such that at $T=1.8$ the CSPA potential at $\gamma=0$ still exhibits a shallow prolate minimum. For higher T the RPA effects are nevertheless negligible. As γ increases, the well at $\beta>0$ (<0) becomes shallower (deeper), approaching of course a symmetric potential at $\gamma=\pi/6$.

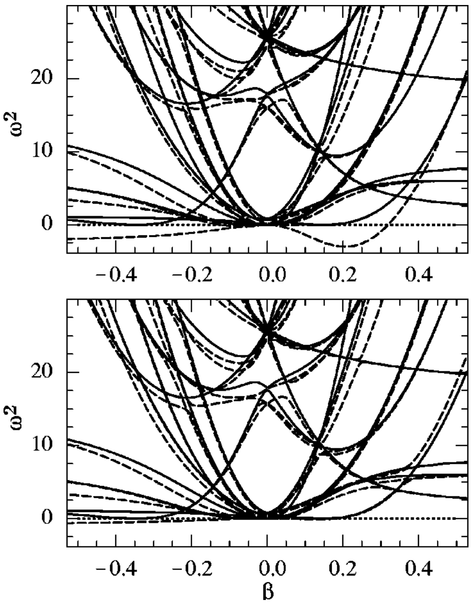

FIG. 4. Square of the RPA energies (in MeV^2) as a function of deformation for $\gamma=0$, at $T=1$ MeV (top) and $T=1.8$ MeV (bottom). Dashed ines depict the square of the pair energies ε_2 in Eq. (9).

In the lower panel we compare the exact canonical value of F_{SPA} with the saddle point approximation (23)

$$F_{\mathrm{SPA}}(\tilde{x}) \approx -T \ln \prod_{\tau} (z_0^\tau)^{-N_\tau} Z_\tau(\tilde{x}, z_0^\tau)/(2\pi\sigma_{N_\tau}^2)^{1/2}, \tag{55}$$

with $z_0^\tau(\tilde{x})$ determined *for each* $\tilde{x}$ by the constraint $\Sigma_k p_k(z_0^\tau)=N_\tau$ [Eq. (22)]. Results are almost coincident except for the region of large β (of small thermodynamic weight) where the average SP level spacing is larger than T (as seen for $T=1$ MeV and $\beta>0.5$). There is, however, a non-negligible difference with the ordinary GC free energy potential, obtained neglecting the fluctuation in Eq. (55), i.e., setting $z_0^\tau=e^{\beta\mu_\tau}$,

$$F_{\mathrm{SPA}}(\tilde{x}) \approx \sum_{\tau} -T \ln Z_\tau(\tilde{x}, \mu_\tau) + \mu_\tau N_\tau, \tag{56}$$

whose minimum determines the GC mean field [Eqs. (45) with p_k the Fermi probability $p_k(z_0)$]. At fixed T, the number fluctuations $\sigma_{N_\tau}^2$ are larger for small deformations (due to the smaller level spacing) and increase the actual canonical free energy for small β, unfavoring the spherical shape and increasing T_c in the canonical case. Moreover, due to this effect the canonical potential develops a very flat maximum between the spherical and prolate minima for T just below T_c, which disappears together with the prolate minimum at $T=T_c$, making the final transition first order. These effects can also be seen through the probabilities p_k, which in the canonical case are smaller (larger) than in the GC case at the same T for levels above (below) the Fermi level, leading to a retardation of thermal effects.

The important effects of the measure $m(\tilde{x})$ in Eq. (36) are seen in Fig. 3, which depicts the normalized distributions

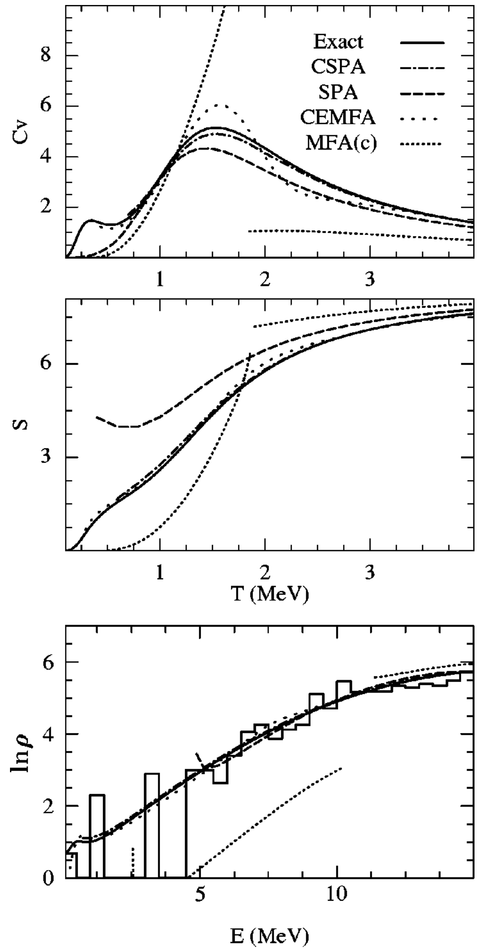

FIG. 5. Specific heat $C_v=dE/dT$ (top) and canonical entropy $S=\ln Z+E/T$ (center) vs temperature according to exact, CSPA, SPA, CEMFA, and canonical MFA results. Bottom: The logarithm of the corresponding level densities (in MeV^{-1}) obtained from the saddle point approximation (58) as a function of excitation energy. The exact microcanonical result is also depicted.

$$P(\tilde{x}) \propto Z(\tilde{x}) m^\sigma(\tilde{x}), \tag{57}$$

where the ''intrinsic'' distribution corresponds to $\sigma=0$ whereas the actual one to $\sigma=1$. At low T there are no significant differences, but at $T=1.8$ MeV, the first one becomes flat around $\beta=0$ while the second remains peaked at $\beta\neq 0$, exhibiting an approximate Gaussian shape for all T which justifies the effective mean field approach (49).

Figure 4 depicts the squared RPA energies at fixed T for $\gamma=0$. The largest contribution to the RPA correction for $T<T_c$ is provided by the two lowest modes (continuation of the Goldstone modes for arbitrary β,γ), which for $\gamma=0$ are degenerate and vanish at the self-consistent mean field, becoming imaginary for smaller and oblate deformations. The largest imaginary value is actually attained at a triaxial shape. For $T=1.8$ MeV the lowest mode is still imaginary for oblate as well as nearby triaxial shapes, although for high T all modes become real. They are also real for large $|\beta|$ at any T, except for strictly axial shapes (of no weight in the CSPA integral). The canonical effects on the RPA energies are small and visible mainly in the two lowest modes, as they

vanish at self-consistent mean field of the ensemble considered. The main consequence is a retardation of thermal effects.

Finally, we depict in Fig. 5 the specific heat $C_v = dE/dT$, the canonical entropy $S=\ln Z+E/T$ and the level density obtained in the saddle point approximation

$$\rho(E)=e^S/\sqrt{2\pi T^2 C_v}, \tag{58}$$

where $E=-\partial \ln Z/\partial T^{-1}$. CSPA results are almost exact for all quantities above the breakdown temperature, while those from the effective mean field approximation (49) provide an accurate estimate of the entropy and level density. The SPA results are not accurate at low T, although its prediction of the level density is correct when plotted in terms of the corresponding energy. Note, however, that none of the present approximations is able to describe the low T peak in the exact C_v at $T\approx 0.25$ MeV (below the CSPA breakdown) which is due to the comparatively small energy difference between the ground and first excited states ($J^\pi=0^+$ and 2^+). This effect could be described in principle by applying angular momentum projection (see Ref. [6] for angular momentum projected SPA).

For completeness, we have also plotted, in addition to the exact smoothed level density determined by Eq. (58), the exact *microcanonical* level density for an energy bin of 0.5 MeV, whose average agrees well with Eq. (58) for excitation energies above 5 MeV. In this region all approximations, except for the mean field, yield an accurate prediction of the average density.

IV. CONCLUSIONS

We have formulated the CSPA and mean-field+RPA in a general form which enables a direct implementation in a canonical ensemble for a standard density decomposition of a two-body interaction. The canonical formalism does not imply a significant increase in numerical effort in comparison with the GC treatments. The excellent agreement with the exact canonical results for a quadrupole interaction indicate that a high degree of accuracy can be achieved with the canonical CSPA. Moreover, we have also developed in this case a simple effective saddle-point approximation to the CSPA, which practically reproduces the CSPA results for level densities and first derivatives of the PF without any integration, and which can be extended to lower temperatures. The present techniques pave the way for an application of the CSPA to more realistic forces, where use of the approximation (27) for variables associated with repulsive or weak attractive terms would help to reduce the final number of integration variables. Finally, we remark that all present methods are easily applicable within large configuration spaces, as the RPA correction can be evaluated with Eq. (8) without explicitly determining the RPA energies.

ACKNOWLEDGMENTS

N.C. and R.R. wish to thank CONICET and CICPBA of Argentina for financial support, and wish to thank the hospitality of the Physik-Department der Technischen Universität München. Work supported in part by the EEC (Contract No. CII*-CT93-0352).

APPENDIX A

The response matrix in Eq. (8) is given in general by

$$R_{\nu\nu'}(x,\omega)=\delta_{\nu\nu'}+v_\nu \sum_{K\neq K'} \langle K|Q_\nu|K'\rangle \times\langle K'|Q_{\nu'}|K\rangle \frac{P_K-P_{K'}}{E_K-E_{K'}+\omega} \tag{A1}$$

(see Ref. [15]), where $|K\rangle$ are the many-body eigenstates $H(x)|K\rangle=E_K|K\rangle$ and $P_K=e^{-\beta E_K}/Z(x)$ the corresponding probabilities, with $Z(x)=\Sigma_K e^{-\beta E_K}$ the PF. The ensemble considered is assumed to be a *closed* representation of the operators Q_ν. If H_0 and Q_ν are one-body operators of the form (10),(11), and the eigenstates in the ensemble considered are independent particle states $|K\rangle=\Pi_k a_k^\dagger|0\rangle$ the sum in Eq. (A1) becomes

$$\sum_{k\neq k'} \frac{\tilde{Q}^{\nu}_{kk'}\tilde{Q}^{\nu'}_{k'k}}{\varepsilon_k-\varepsilon_{k'}+\omega} \sum_K P_K\langle K|n_k(1-n_{k'})-n_{k'}(1-n_k)|K\rangle,$$

where $n_k\equiv a_k^\dagger a_k$, which leads then to Eq. (12) with

$$p_k\equiv\sum_K P_K\langle K|n_k|K\rangle,$$

the probabilities (13). In a canonical ensemble with a fixed number of proton and neutrons, these expressions are then valid for operators H_0, Q_ν which conserve both the proton and neutron particle numbers.

We also obtain the general expressions

$$-\frac{v_\nu}{\beta}\frac{\partial \ln Z(x)}{\partial x_\nu}=x_\nu-v_\nu\langle Q_\nu\rangle_x,$$

$$-\frac{v_\nu}{\beta}\frac{\partial^2 \ln Z(x)}{\partial x_\nu \partial x_{\nu'}}=\delta_{\nu\nu'}+v_\nu R^0_{\nu\nu'}(x), \tag{A2}$$

where $\langle Q_\nu\rangle_x=\Sigma_K P_K\langle K|Q_\nu|K\rangle$ and

$$R^0_{\nu\nu'}(x)=\sum_{K\neq K'}\langle K|Q_\nu|K'\rangle\langle K'|Q_{\nu'}|K\rangle\frac{P_K-P_{K'}}{E_K-E_{K'}} -\beta\left(\sum_K P_K\langle K|Q_\nu|K\rangle\langle K|Q_{\nu'}|K\rangle-\langle Q_\nu\rangle\langle Q_{\nu'}\rangle\right). \tag{A3}$$

In the case of one-body operators and independent particle states $|K\rangle$, Eq. (A3) leads to Eq. (29).

APPENDIX B

In order to derive Eq. (30), we consider in general

$$\langle a_k^\dagger a_k a_{k'}^\dagger a_{k'}\rangle\equiv Z^{-1}\mathrm{Tr}[Pe^{-\beta h}a_k^\dagger a_k a_{k'}^\dagger a_{k'}], \tag{B1}$$

where $h=\Sigma_k \varepsilon_k a_k^\dagger a_k$, $Z=\mathrm{Tr}\, P e^{-\beta h}$, with Tr the GC trace and P a projector onto a restricted ensemble. As

$$e^{-\beta h} a_k^\dagger a_k a_{k'}^\dagger a_{k'} = e^{-\beta h} a_k^\dagger a_k + a_k^\dagger a_{k'} e^{-\beta(\varepsilon_k - \varepsilon_{k'} + h)} a_k a_{k'}^\dagger ,$$

we obtain, *provided* $[P, a_k^\dagger a_{k'}]=0$,

$$\langle a_k^\dagger a_k a_{k'}^\dagger a_{k'} \rangle = p_k + e^{-\beta(\varepsilon_k - \varepsilon_{k'})}[\langle a_k^\dagger a_k a_{k'}^\dagger a_{k'} \rangle - p_{k'}],$$

where $p_k = \langle a_k^\dagger a_k \rangle$. If P is the projector onto fixed proton and neutron particle number, this holds for k and k' of the same isospin. We obtain then Eq. (30) when $\varepsilon_k \neq \varepsilon_{k'}$.

[1] J. Hubbard, Phys. Rev. Lett. **3**, 77 (1959); R. L. Stratonovich, Dokl. Akad. Nauk. SSSR **115**, 1097 (1957) [Sov. Phys. Dokl. **2**, 416 (1958)].
[2] B. Mühlschlegel, B. Scalapino, and D. J. Denton, Phys. Rev. B **6**, 1767 (1972).
[3] Y. Alhassid and J. Zingman, Phys. Rev. C **30**, 684 (1984).
[4] P. Arve, G. F. Bertsch, B. Lauritzen, and G. Puddu, Ann. Phys. (N.Y.) **183**, 309 (1988); B. Lauritzen, P. Arve, and G. F. Bertsch, Phys. Rev. Lett. **61**, 2835 (1988).
[5] Y. Alhassid and B. Bush, Nucl. Phys. **A549**, 43 (1992).
[6] R. Rossignoli, A. Ansari, and P. Ring, Phys. Rev. Lett. **70**, 9 (1993); R. Rossignoli and P. Ring, Ann. Phys. (N.Y.) **235**, 350 (1994).
[7] L. G. Moretto, Phys. Lett. **40B**, 1 (1972).
[8] A. L. Goodman, Phys. Rev. C **29**, 1887 (1984); **37**, 2162 (1988).
[9] J. L. Egido, P. Ring, S. Iwasaki, and H. J. Mang, Phys. Lett. **154B**, 1 (1985).
[10] G. Puddu, P. F. Bortignon, and R. A. Broglia, Ann. Phys. (N.Y.) **206**, 409 (1991); Phys. Rev. C **42**, 1830 (1990).
[11] B. Lauritzen, G. Puddu, P. F. Bortignon, and R. A. Broglia, Phys. Lett. B **246**, 329 (1990).
[12] G. Puddu, Phys. Rev. C **47**, 1067 (1993).
[13] H. Attias and Y. Alhassid, Nucl. Phys. **A625**, 363 (1997).
[14] R. Rossignoli and N. Canosa, Phys. Lett. B **394**, 242 (1997); Phys. Rev. C **56**, 791 (1997).
[15] R. Rossignoli and P. Ring, Nucl. Phys. **A633**, 613 (1998).
[16] C. W. Johnson, S. E. Koonin, G. H. Lang, and W. E. Ormand, Phys. Rev. Lett. **69**, 3157 (1992); G. H. Lang, C. W. Johnson, S. E. Koonin, and W. E. Ormand, Phys. Rev. C **48**, 1518 (1993).
[17] S. E. Koonin, D. J. Dean, and K. Langanke, Phys. Rep. **278**, 1 (1997).
[18] R. Rossignoli, N. Canosa, and J. L. Egido, Nucl. Phys. **A605**, 1 (1996); **A607**, 250 (1996).
[19] A. K. Kerman, S. Levit, and T. Troudet, Ann. Phys. (N.Y.) **148**, 436 (1983).
[20] R. Rossignoli, N. Canosa, and P. Ring, Phys. Rev. Lett. **72**, 4070 (1994).
[21] M. Brack, O. Genzken, and K. Hansen, Z. Phys. D **21**, 65 (1991).
[22] J. L. Egido and O. Rasmussen, Nucl. Phys. **A476**, 48 (1988).